ISSN 1070-4272, Russian Journal of Applied Chemistry, 2009, Vol. 82, No. 1, pp. 86−93. © Pleiades Publishing, Ltd., 2009.
Original Russian Text © P.A. Nikul'shin, N.N. Tomina, Yu.V. Eremina, A.A. Pimerzin, 2009, published in Zhurnal Prikladnoi Khimii, 2009, Vol. 82, No. 1, pp. 86−93.

ORGANIC SYNTHESIS AND INDUSTRIAL ORGANIC CHEMISTRY

Use of $(NH_4)_4[Ni(OH)_6Mo_6O_{18}]\cdot nH_2O$ Heteropoly Compound in Fabrication of Sulfide Catalysts for Hydropurification of Diesel Fractions

P. A. Nikul'shin, N. N. Tomina, Yu. V. Eremina, and A. A. Pimerzin

Samara State Technical University, Samara, Russia

Received September 17, 2008

Abstract—NiMo(S)/γ-Al_2O_3 hydropurification catalysts were synthesized using as a precursor the active sulfide phase of a heteropoly compound with Anderson structure, ammonium 6-molybdonickelate, and, for comparison, ammonium paramolybdate. The heteropoly compound synthesized was identified using X-ray phase analysis and IR spectroscopy and its thermal stability was analyzed with DTA. The hydrodesulfurizing and hydrogenating activity of catalysts synthesized from ammonium 6-molybdonickelate was examined in hydropurification of two diesel fractions with different contents of polycyclic aromatic hydrocarbons and close contents of sulfur.

DOI: 10.1134/S1070427209010169

The practice of last decades shows that the demand of oil processing industries for new effective hydropurification catalysts has been steadily increasing. This rise is due to the deterioration of the quality of raw materials for hydropurification and to increasingly stringent requirements imposed on processing products. For example, Euro-4 motor fuel standards with more stringent requirements to the content of sulfur and aromatic hydrocarbons have been in force in European Union (EU) countries since 2005 [1].

Because diesel engines are promising for automobile transportation, steadily increasing attention has been given to the ecological safety of diesel fuels (DF) in recent years; the XXI century is declared the century of low-sulfur DF [2]. According to [3, 4], all vehicles with diesel engines will run in Europe on ultra-low-sulfur diesel (ULSD) fuel in the future. In addition, the EU intends to introduce a new requirement to the content of sulfur in diesel fuel and gasoline, so that all diesel vehicles should be converted by 2010 to the near-zero-sulfur diesel (NZSD) fuel.

The necessity for organization of a mass production of DF with low sulfur content in Russia is beyond any doubt and is determined not only by ecological requirements. After entry into WTO, Russia will be required to observe standards of this organization, including ecological management ISO standards of 1400 series.

The quality of the raw materials for DF hydropurification becomes poorer because of the deterioration of oil quality and involvement of secondary distillates. The secondary distillates are more difficultly subject to hydrogenation processing than straight-run fractions because of the presence of a substantially larger amount of difficultly removable sulfur compounds with cyclic structure, polycyclic aromatic hydrocarbons (PAH), unsaturated hydrocarbons, and tarry substances [5]. Domestic industrial hydropurification catalysts are inferior to their foreign analogues and give no way of manufacturing an ecologically pure DF on industrial installations even upon making the technological mode substantially more stringent. Under these conditions, development of new catalysts with enhanced hydrodesulfurizing (HDS) and hydrogenating (HYD) activity is a topical task.

In this study, the possibility of using a molybdenum heteropoly compound (HPC) with Anderson structure as a precursor of the active phase of the catalyst for hydropurification of diesel fractions was examined experimentally.

EXPERIMENTAL

$(NH_4)_4[Ni(OH)_6Mo_6O_{18}]\cdot nH_2O$ (ammonium 6-molybdonickelate, henceforth $NiMo_6$-HPC) was synthesized

Table 1. Parameters of the catalysts synthesized

Sample	Content in catalyst, wt %						
	Mo	Ni	S	after tests*			
				sulfur		coke	
				raw material 1	raw material 2	raw material 1	raw material 2
APM	10.0	3.1	4.0	4.8	4.8	3.1	2.1
$NiMo_6$–HPC	9.9	3.1	5.1	6.6	4.9	1.5	1.4

* Test on a flow-through installation for 12 h.

Table 2. Physicochemical properties of the diesel fractions used

Sample	ρ_4^{20}, g cm^{-3}	n_4^{20}	Content in hydrogenation product, wt %		
			sulfur	BAH*	TAH*
Raw material 1 (4.83)**	0.8377	1.4670	1.113	3.69	1.14
Raw material 2 (14.01)	0.8779	1.4915	1.090	9.64	4.37

* BAH, bicyclic aromatic hydrocarbons; TAH, tricyclic aromatic hydrocarbons.
** PAH content (BAH + TAH, wt %) is given in parentheses.

by the known procedures [6, 7]. To confirm the structure of $NiMo_6$-HPC, its Mo and Ni contents were determined spectrophotometrically, its IR spectra were measured on Avatar 360 instrument (Fig. 1), and its phase composition was found on a DRON-2 X-ray diffractometer (CuKα radiation). The NiMo6-HPC and $(NH_4)_6Mo_7O_{24}\cdot 4H_2O$ (ammonium paramolybdate, APM) obtained were subjected to differential-thermal analysis (DTA) on a DSK-500 differential scanning calorimeter (Fig. 2). IR spectra of NiMo6-HPC were measured after its calcination at different temperatures (Fig. 3).

γ-Al_2O_3 synthesized by the method described in [8] served as a catalyst support. The texture characteristics of the aluminum oxide prepared were determined by measuring the adsorption of nitrogen at a temperature of 77 K on a Micromeritics ASAP 2020 adsorption porosimeter. The specific surface area of the aluminum oxide was 315 m^2 g^{-1}, and the effective pore diameter, 110 Å.

Nickel-promoted NiMo(S)/γ-Al2O3 catalysts based on NiMo6-HPC were prepared by impregnating a support to its moisture capacity with a solution of HPC and $Ni(NO_3)_2$ $6H_2O$ (analytically pure grade). No precipitation from joint solutions of nickel nitrate and HPC was observed for 24 h, which made it possible to introduce Ni and Mo compounds in a single impregnation stage. As a reference sample served NiMo(S)/γ-Al_2O_3 catalyst prepared from APM and nickel nitrate. The calculated content of MoO_3 in the catalysts was 15 wt %, and that of NiO, 4 wt %. The finished catalysts were dried at temperatures of 80, 100, and 120°C (2 h at each temperature), then the temperature was raised at a rate of 1 deg min^{-1} to 400°C

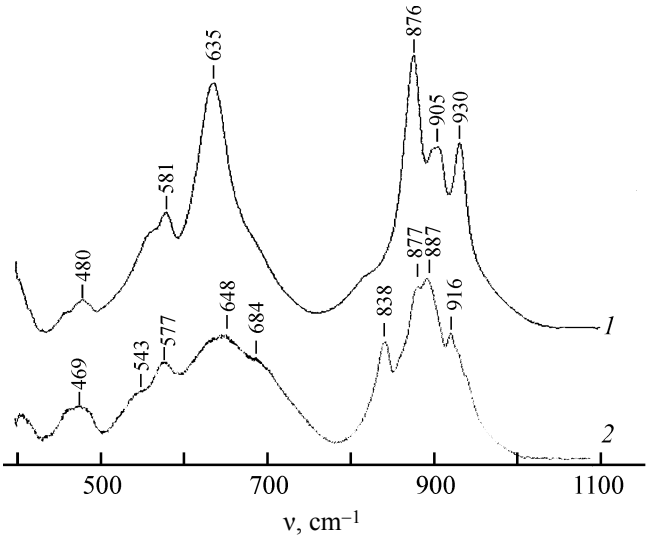

Fig. 1. IR spectra of (*1*) NiMo6-HPC and (*2*) APM dried at 110°C. (ν) Wave number; the same for Fig. 3.

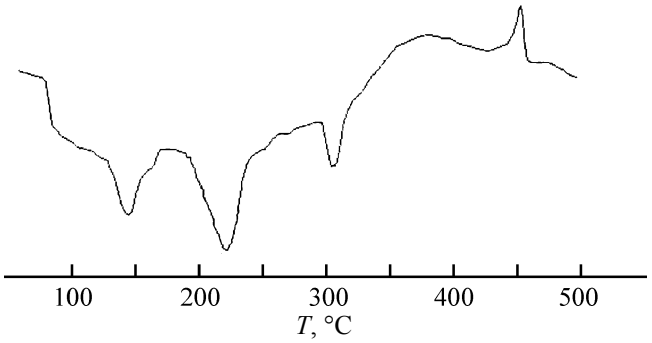

Fig. 2. DTA curve of $NiMo_6$-HPC. (*T*) Temperature.

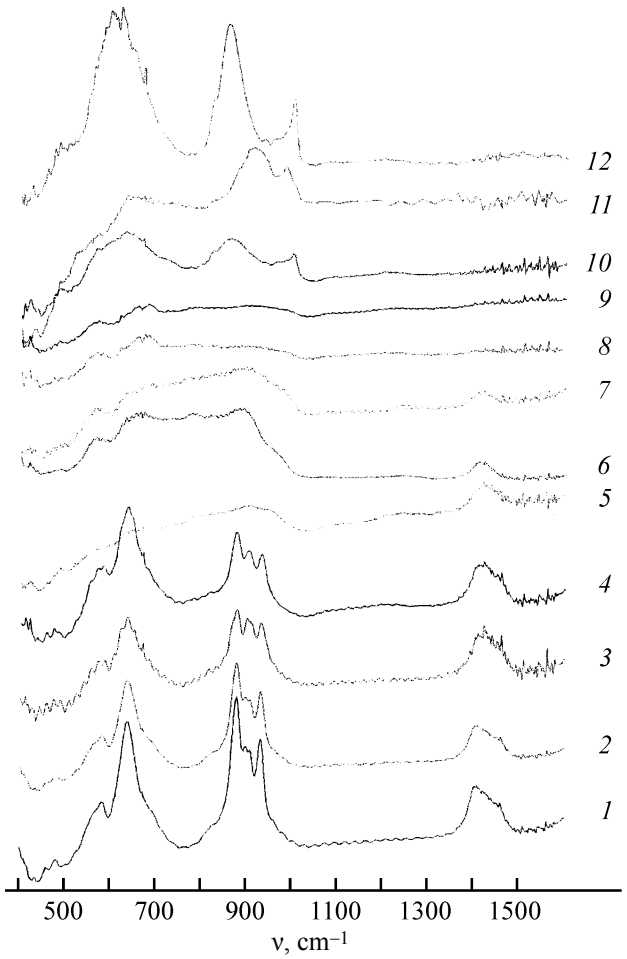

Fig. 3. IR spectra of $NiMo_6$-HPC dried and calcined at different temperatures. *T* (°C): (*1*) 125, (*2*) 140, (*3*) 175, (*4*) 180, (*5*) 225, (*6*) 250, (*7*) 299, (*8*) 310, (*9*) 325, (*10*) 400, (*11*) 450, (*12*) 550.

and the catalysts were calcined for 2 h. Then the catalyst obtained in the oxide form was subjected to sulfidation. For this purpose, the 0.25–0.50-mm fraction of the catalyst was impregnated with the sulfidizing agent, di-*tert*-butyl polysufide (sulfur content 54 wt %), placed in a separate glass reactor, and sulfidized under a hydrogen pressure of 101 kPa for 2 h at a temperature of 350°C. The content of active elements in the catalysts was monitored by photocolorimetry; the content of sulfur before and after tests in a flow-through installation was determined by the method similar to that described in [9] (Table 1).

The sulfidized catalysts were tested on a laboratory flow-through installation in hydropurification of two diesel fractions whose physicochemical parameters are listed in Table 2. Raw material 1: straight-run diesel fuel; raw material 2: mixture of 50% straight-run diesel fuel and 50 vol % light gas oil produced by catalytic cracking. The tests were performed under the following conditions: temperature 320, 340, 360, and 380°C; pressure 4.0 MPa; volumetric flow rate of the raw material 2.0 l h^{-1}; hydrogen : raw material ratio 600 nl/l; catalyst volume 10 cm^3.

The total sulfur content in the raw materials and hydrogenation products was determined using the lamp method and X-ray fluorescence (on a Shimadzu EDX800HS) technique. The content of PAHs was found with a Shimadzu UV-1700 spectrophotometer [10, 11]. The activity of the catalysts was evaluated by a decrease in the contents of sulfur (HDS activity) and PAHs (HYD activity) in the hydrogenation products obtained after purification on a flow-through installation, compared with those in the raw material.

The content of coke in spent catalysts was found by its quantitative oxidation to CO_2, followed by gas-chromatographic analysis (Table 1).

To identify the NiMo6-HPC obtained and analyze the possibility of its use to fabricate hydropurification catalysts, the physicochemical properties of this compound were examined. According to the results of a quantitative analysis, the Mo/Ni atomic ratio in the compound is about 6. Figure 1 shows IR spectra of the NiMo6-HPC synthesized and APM. The characteristic bands of the Anderson HPC coincide with those reported previously [12–16]. The strong absorption bands at 880–950 cm-1 are associated with cis-MoO_2 bonds, and those at 450–650 cm^{-1}, with Mo–O–Mo bridge bonds (Fig. 4). An X-ray phase analysis of NiMo6-HPC demonstrated that the compound has a complex crystal structure. Its interplanar spacings coincide with published data [17, 18]. The whole body of data (results of quantitative analysis, IR spectroscopy, and X-ray phase analysis) demonstrated that the compound synthesized is a sixth row HPC of Anderson structure.

The decomposition point is a fundamental parameter of any chemical compound, including HPC. Because of the difficult identification of thermolysis products, determining the instant of HPC decomposition is frequently problematic. Fabrication of hydropurification catalysts includes such thermal stages as drying and calcination. The degree of sulfidization and, possibly, the activity of a catalyst depend on which molybdenum compounds are present on the catalyst surface after calcination and before sulfidization.

The thermal decomposition of HPC occurs in stages with splitting-off of water and ammonia and with the final separation of two (or more, depending on the nature

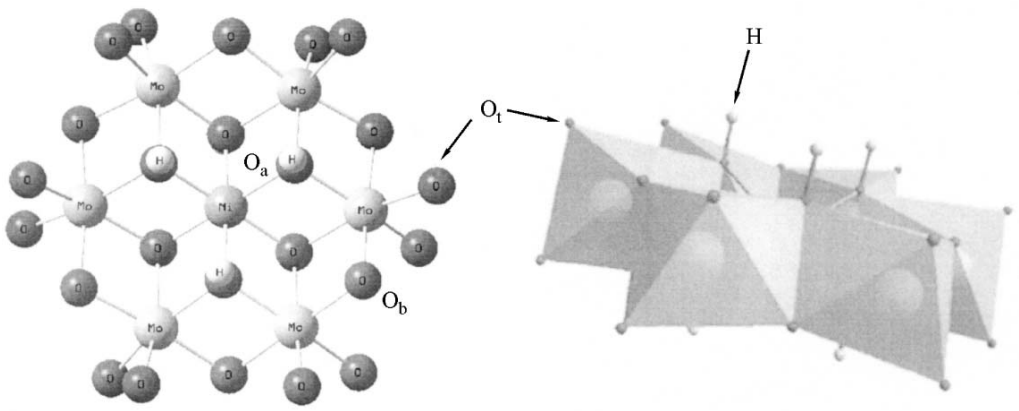

Fig. 4. Representation of the $[NiII(OH)_6Mo_6O_{18}]_4$- anion in the protonated form of the Anderson structure (left, bonds; right, polyhedral model adapted from [20]). O_a is the bridge oxygen atom with a coordination number of 3, connects to Mo atoms and atom of the hetero-element Ni; O_b, bridge oxygen atom with a coordination number of 2, connects two Mo atoms; O_t, terminal (end or "-yl" oxygen atom. The figure shows six hydrogen atoms bonded to six oxygen atoms O_a to give "constitution water."

of HPC) oxide phases, as a rule, at high temperatures [12–14]. Comparison of DTA data and IR spectra of HPC enables analysis of changes occurring with a compound subjected to a thermal treatment.

It can be seen from the data in Fig. 2 that the DTA curve of $NiMo_6$–HPC has three endothermic peaks at 140, 210, and 300°C. The endothermic effects observed on heating the compound can be attributed to rupture of the existing bonds, which consumes energy, or to evaporation processes.

Figure 3 shows IR spectra of NiMo6-HPC dried and calcined at different temperatures. Comparison of the IR spectra with the DTA curve (Fig. 2) suggests the following. At a temperature of 140°C, crystal water is split-off, because the relative intensity of the characteristic band at 1400 cm^{-1} (Fig. 3), associated with deformation vibrations of the ammonium ion, is preserved and the relative intensity of the band at 3400 cm^{-1} (not shown in Fig. 3), associated with vibrations of water molecules, decreases.

In the temperature range above 220°C, structural changes occur in HPC, which reflects on the nature of IR spectra of $NiMo_6$-HPC dried at 225°C and higher. The relative intensity of the characteristic band at 1400 cm^{-1} remains nearly unchanged. Thus, the endothermic effect at 210°C is accounted for by the loss of constitution water bound to the central octahedron of the heteroatom in the form of OH groups, rather than by release of ammonia (Fig. 4). The replicas at 530–700 cm^{-1} (Fig. 3), associated with Mo–O–Mo vibrations, remain at any of the drying and calcination temperatures. The endothermic peak at 300°C is associated with the release of ammonia, because the band at 1400 cm^{-1} in the IR spectrum of HPC disappears in this case. The DTA curve also shows an exothermic peak at 440°C. This peak may be associated with rearrangement of Ni–O–Mo and Mo–O–Mo bonds in the heteropoly anion, with a more stable structure formed. At HPC calcination temperatures of 400–550°C, new characteristic bands, close in relative intensity to those of MoO_3, appear in the IR spectra of thermolysis products in the range 800–900 cm^{-1} (Fig. 3). However, comparison with the IR spectra of individual MoO_3 shows that these bands are shifted to longer wavelengths. This possibly indicates that the crystal structure of MoO_3 formed in HPC calcination is distorted via incorporation of Ni into this compound.

It has been shown previously that thermal decomposition of an HPC derived from the Anderson structure, ammonium dodecamolybdodicobaltate(II) $(NH_4)_6[Co_2Mo_{10}O_{38}H_4]$ [$7H_2O$, at 750°C yields cobalt molybdate $CoMoO_4$ [21]. Upon calcination of NiMo6-HPC at 550°C, no characteristic bands of individual NiMoO4 have been found by IR spectroscopy [13].

Of interest in the present study is, primarily, the conversion of HPC at temperatures of up to 400°C, because this temperature is the highest used in calcination of the catalyst in the course of its fabrication. The results of the study suggest the following: below 400°C, the structure of the heteropoly anion is not disintegrated even upon heating of a "free" compound unbound to a support. It has been shown previously [22] that HPC supported by Al_2O_3 has a substantially higher thermal stability, and, consequently, supported $NiMo_6$-HPC will preserve its structure in some way and will thereby retain the active

components in close molecular contact in the oxide form of the catalysts.

To study mixed phases formed on the aluminum oxide surface after deposition of salts of the active components, drying, calcination, and sulfidization, an X-ray phase analysis of the catalysts synthesized was made and their IR spectra were measured. The IR spectra of the catalysts in the oxide form have no characteristic bands, and the broadened band at 500–1500 cm^{-1} is typical of γ-Al_2O_3. The X-ray diffraction patterns of the oxide and sulfide catalysts also exhibited only the X-ray-amorphous low-temperature γ-Al_2O_3 phase with d/n = 1.971 and 1.401 Å. The X-ray phase analysis did not reveal any bulk sulfides (the samples are X-ray amorphous in all crystallographic directions, i.e., the coherent scattering region does not exceed 20 Å, and, therefore, it can be suggested that the active phase of the catalysts is in the ultradispersed state [23, 24].

The content of the active components in the catalysts is nearly the same (Table 1), which makes correct their comparison. It has been shown previously [25] that the degree of sulfidization of Ni and Mo correlates with the activity of these catalysts in hydrogenolysis of thiophene. The sulfur content of the catalysts can be used to estimate the degree of sulfidization of the active components: in the samples synthesized it is lower than 100%, being about 50 rel % for catalysts based on AMP and 62 rel % for those based on NiMo6-HPC. This means that molybdenum oxysulfides are formed on the surface of aluminum oxide. The degree of sulfidization of the active components is higher for sample 2, because Mo in the heteropoly anion is more easily reduced owing to the donor properties of the heteroatom [21, 26].

The dependence of the HDS activity of the catalysts on the temperature of hydropurification of raw materials 1 and 2 (Table 2) is shown in Fig. 5, whence can be seen that the NiMo6-HPC catalysts exhibit a higher activity over the entire temperature range, compared with AMP catalysts (at 320°C, the difference is 15.8 rel % for raw material 1 and 16.3 rel % for raw material 2, which is equivalent to a 2.3–2.5-fold decrease in the sulfur content of hydrogenation products) for both types of raw materials.

The dependence of the HYD activity of the catalysts on the testing temperature is shown for raw materials 1 and 2 in Fig. 6. $NiMo_6$-HPC catalysts are also more active in the entire temperature range than APM catalysts. In tests with raw material 1, the difference is (rel %) 24.4 at 320°C, 19.5 at 340°C, 0.6 at 360°C, and 4.7 at 380°C. In tests with raw material 2, the difference is (rel %) 14 at 320°C, 15.4 at 340°C, 4.6 at 360°C, and 3.7 at 380°C.

The activity in hydrodesulfurization and hydrogenation of PAH in the diesel fraction well correlates with the amount of coke deposits (Figs. 5, 6; Table 1). The $NiMo_6$-HPC catalysts, the most active in hydrogenation, contain a smaller amount of coke (after tests, the content of coke is 0.7 wt % lower for raw material 1, and 1.6 wt % lower for raw material 2), which is accounted for by the better hydrogenation of coke precursors on these catalysts. A combination of the maximum hydrogenating activity of the catalysts with the minimum carbidization has already

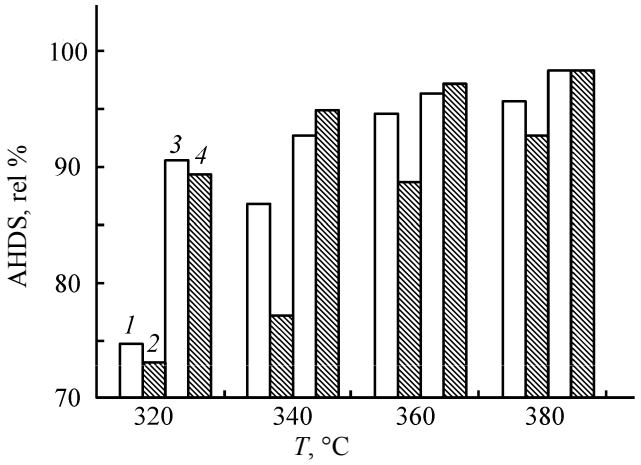

Fig. 5. HDS activity of catalysts fabricated using (*1, 2*) APM and (*3, 4*) $NiMo_6$-HPC vs. the temperature of hydropurification of raw material (*1, 3*) 1 and (*2, 4*) 2. (AHDS) Hydrodesulfurizing activity of a catalyst and (*T*) temperature.

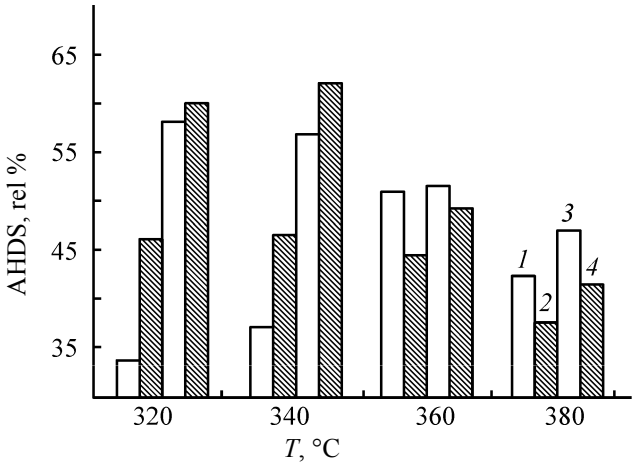

Fig. 6. HYD activity of catalysts fabricated using (*1, 2*) APM and (*3, 4*) $NiMo_6$-HPC vs. the temperature of hydropurification of raw material (*1, 3*) 1 and (*2, 4*) 2. (AHYD) Hydrogenating activity of a catalyst and (*T*) temperature.

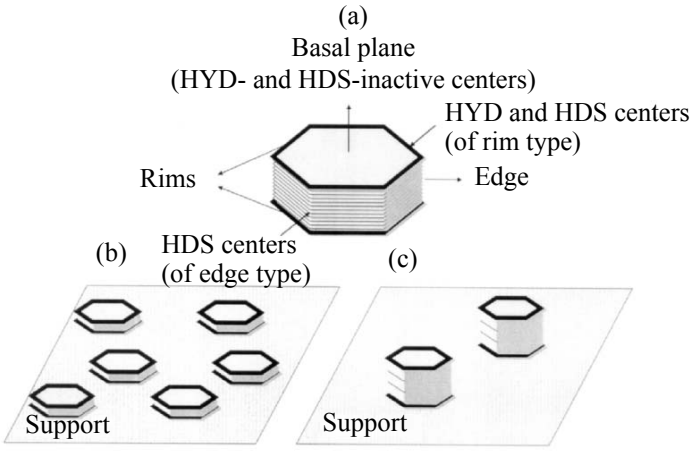

Fig. 7. Catalytically active centers of catalysts based on (a) MoS_2 and active NiMoS phases (b) I and (c) II.

been noted for aluminonickelmolybdenum catalysts [8, 27, 28].

Comparison of the HDS and HYD activities of the catalysts demonstrates that the PAH concentration in different kinds of raw materials affects the results obtained. The higher content of PAH in raw material 2, compared with raw material 1, at close contents of sulfur, results in that the conversion of sulfur-containing compounds on the APM catalyst decreases. This can be explained, first, from the standpoint of competition for active centers of the phase between sulfur-containing molecules and molecules of polycyclic aromatic compounds. Second, the APM catalysts lose activity because of the enhanced formation of coke blocking the active centers of desulfurization, which is due to the low hydrogenating activity of the catalyst. As the PAH concentration in a raw material increases, the content of coke in spent catalysts becomes higher (Table 1). With APM catalysts, the content of coke is 2.1 wt % for raw material 1 (with low content of PAH) and 3.1 wt % for raw material 2 (with higher content of PAH). In $NiMo_6$–HPC catalysts, the increase in the amount of coke is insignificant (0.1 wt %).

The conversion of sulfur-containing compounds on NiMo6-HPC catalysts does not decrease when raw materials with high PAH content are used, which may point to a larger amount of accessible active centers of the sulfide "NiMoS" phase in this catalyst (at the same content of Mo and Ni). The data obtained can be accounted for by formation of a more geometrically advantageous multilevel active NiMoS phase of type II on the support surface. On this phase, desulfurization and hydrogenation centers exist together and operate in parallel. Indeed, according to the "edge-and-rim" model [29], catalysts formed on the basis of MoS_2 layers have HDS and HYD centers that are identical in structure, but are situated on, respectively, "rims" and edges of MoS2 crystallites (Fig. 7a). The centers that are situated at crystallite corners (places of intersection of an edge and a rim) and, by virtue of this circumstance, are coordinationally unsaturated to the greatest extent, are HYD centers. The relative amounts of these canters can be varied by changing the ratio between the diameter and height of a crystallite.

If APMs are used to prepare hydropurification catalysts by the conventional synthesis techniques, it would be expected that a type-I NiMoS phase should be formed (Fig. 7b). At a higher PAH content of raw materials used in the hydropurification process, the HDS activity of such a catalyst will decrease because of the competition of sulfur-containing and aromatic hydrocarbons for active centers (HDS and HYD centers) situated only at the rims of the active phase. By contrast, the NiMoS phase of type II is multilevel, i.e., is constituted by several MoS_2 layers (plates) and contains, in addition to HYD and HDS centers at the rims, also HYD centers on the edges (Figs. 7a, 7c). In this case, an increase in the PAH content on the hydropurification raw material will not affect, up to certain values, the HDS activity of the catalyst because the competition between the sulfur-containing and aromatic hydrocarbons will be compensated for by the presence of HDS centers on the edges.

The catalyst lifecycle model suggested in [31] includes a scheme of formation of a multilevel sulfide phase from separate layers of molybdenum disulfide. This scheme is operative, e.g., at high sulfidization temperatures.

However, some researchers believe that this model fails to reflect processes occurring in calcination and sulfidization of catalysts. First, metal sulfides are not volatile [24], and, second, the donor properties of a promoter will hinder association of layers of a type-I sulfide phase.

Probably, for creating such a multilevel active sulfide phase, it is necessary to obtain on the surface of an oxide catalyst a precursor that would contain a considerable number of atoms of the main active component (Mo) molecularly bound to the promoter (Ni). In the course of sulfidization, this oxide precursor is converted to a multilevel sulfide phase and the promoter does not migrate into the bulk of the support in thermal stages of catalyst fabrication, so that poorly catalytically active spinels $NiAl_2O_4$ are not formed. In this study, the role of such a compound was played by $NiMo_6$-HPC, which, as shown above, does not decompose into separate oxides under a thermal treatment. The high HDS activity of the catalysts synthesized on the basis of $NiMo_6$-HPC does not decrease as the PAH content of raw materials increases, in contrast to APM catalysts, and the rise in the amount of coke on passing to a more aromatized raw material is insignificant.

CONCLUSIONS

(1) An increase in the concentration of polycyclic aromatic hydrocarbons in the diesel fuels used impairs the hydrodesulfurizing activity of catalysts based on ammonium paramolybdate and leads to a rise in their coke content.

(2) As the content of polycyclic aromatic hydrocarbons increases in the case of catalysts based on ammonium 6-molybdonickelate, the conversion of sulfur-containing compounds does not decrease and the rise in the amount of coke is insignificant.

ACKNOWLEDGMENTS

The authors than Haldor Topsoe A/S company for the financial support.

REFERENCES

1. Leliveld, R.G. and Eijsbouts, S.E., *Catal. Today,* 2008, vol. 130, pp. 183–189.
2. Navalikhina, M.D., Kagan, D.N., and Shpil'rain, E.E., *Modern Motor Fuels: Improvement of Their Ecological and Working Parameters by Development and Application of New Catalysts for the Hydroforming Stage, Preprint of Joint Inst High Temp., Russ. Acad. Sci*., Moscow, 2003, no. 8-472.
3. Krylov, O.B., *Kataliz Prom.*, 2003, vol. 2, pp. 82–85.
4. Nacamura, D. and Silvy, R.P., *Oil Gas J*., 2002, vol. 100, pp. 48–56.
5. Eremina, Yu.V., A *Study of Specific Features of the Hydrodesulfurization and Hydrogenation of Components of Diesel Fractions on Molybdenum-containing Catalysts,* Cand. Sci. Dissertation, Samara, 2006.
6. Nikitina, E.A., *Geteropolisoedineniya* (Heteropoly Compounds), Moscow: Goskhimizdat, 1962.
7. *Rukovodstvo po neorganicheskomu sintezu* (Manual of Inorganic Synthesis), Moscow: Mir, 1986, vol. 6.
8. Nikul'shin, P.A., Eremina, Yu.V., Tomina, N.N., and Pimerzin, A.A., *Neftekhimiya,* 2006, vol. 46, no. 5, p. 371.
9. Rybak, B.M., *Analiz nefti i nefteproduktov* (Analysis of Oil and Oil Products), Moscow: Gostoptekhizdat, 1962.
10. Siryuk, A.G. and Zimina, K.I., *Khim. Tekhnol. Topl. Masel*, 1963, no. 2, pp. 52–56.
11. Tomina, N.N., *Cand. Sci. (Chem.) Dissertation*, Ufa, 1990.
12. Maksimov, G.M., *Usp. Khim.*, 1995, vol. 64, no. 5, pp. 480–486.
13. Kozhevnikov, I.V., *Kataliz geteropolisoedineniyami* (Catalysis with Heteropoly Compounds), Moscow: Znanie, 1985.
14. Pop, M.S., *Geteropoli- i izopolioksometally* (Heteropoly and Isopolyoxo Metals), Novosibirsk: Nauka, 1990.
15. Kazanskii, L.P. and Golubev, A.M., *Khimiya soedinenii Mo(VI) i W(VI)* [Chemistry of Mo(VI) and W(VI) Compounds], Novosibirsk: Nauka, 1979, p. 66.
16. Yurchenko, E.N., *Metody molekulyarnoi spektroskopii v khimii koordinatsionnykh soedinenii i katalizatorov* (Methods of Molecular Spectroscopy in Chemistry of Coordination Compounds and Catalysts), Novosibirsk: Nauka, 1986.
17. Munoz, M., Cabello, C.I., Botto, I.L., et al., *J. Mol. Struct*., 2007, vol. 841, pp. 96–103.
18. Ginesra, A. and Giannetta, F., *Gass. Chim. Ital*., 1968, vol. 98, pp. 1197–1212.
19. Cattier, X., Lambert, J.-F., Kuba, S., et al., *J. Mol. Struct.*, 2003, vol. 656, pp. 231–238.
20. Alizadeh, M.H., Emampour, J.S., Salimi, A.R., and Razavi, H., *Spectrochim. Acta,* Pt. A, 2007, vol. 66, pp. 1126–1132.
21. Cabello, S.A., Cabrerizo, F.M., Alvarez, A., and Thomas, H.J., *J. Mol. Catal. A*, 2002, vol. 186, pp. 89–100.
22. Davydov, A.A. and Goncharova, O.I., *Usp. Khim.*, 1993, vol. 62, no. 2, pp. 118–134.

23. Topsøe, H., Clausen, B.S., and Massoth, F.E., *Hydrotreating Catalysis, in Ser. "Catalysis, Science and Technology,"* Anderson, J.R. and Boudart, M., Eds., Berlin: Springer-Verlag, 1996, vol. 11.
24. Startsev, A.N., *Sul'fidnye katalizatory gidroochistki: sintez, struktura, svoistva* (Sulfide Catalysts for Hydropurification: Synthesis, Structure, Properties), Novosibirsk: Geo, 2007.
25. Coulier, L., de Beer, V.H.J., van Veen, J.A.R., and Niemantsverdriet, J.W., *J. Catal*., 2001, vol. 197, pp. 26–33.
26. Pettiti, I., Botto, I.L., Cabello, C.I., et al., *Appl. Catal. A*, 2001, vol. 220, pp. 113–121.
27. Tomina, N.N., Pimerzin, A.A., Loginova, A.N., et al., *Neftekhimiya,* 2004, vol. 44, no. 4, pp. 274–277.
28. Tomina, N.N., Pimerzin, A.A., Eremina, Yu.V., et al., *Izv. Vyssh. Uchebn. Zaved., Khim. Khim. Tekhnol*., 2005, vol. 48, no. 10, pp. 12–15.
29. Daage, M. and Chianelli, R.R., *J. Catal.*, 1994, vol. 149, no. 2, pp. 414–427.
30. Fan, Y., Lu, J., Shi, G., et al., *Catal. Today*, 2007, vol. 125, pp. 220–228.
31. Eijsbouts, S., *Appl. Catal. A*, 1997, vol. 158, pp. 53–92.